CRATER FORMATION IN SOILS BY RAINDROP IMPACT

HOSSEIN GHADIRI*

Faculty of Environmental Sciences, Griffith University, Nathan, Queensland 4111, Australia

Received 3 January 2003; Revised 3 April 2003; Accepted 26 April 2003

ABSTRACT

The process of crater formation by the impact of water drops on soil, sand and various other target material was studied. Craters of various shapes and sizes were observed on different target materials or conditions, ranging from circumferential depression to completely hemispherical shape. Crater shape was dependent upon target material, its flow stress or shear strength and the presence and thickness of water on the surface. Between 5 and 22 per cent of impact energy was spent on cratering, but the relationship between crater volume and kinetic energy of a raindrop was curvilinear, indicating a lower efficiency of impact energy in removing target material as the energy increases. Impact impulse, on the other hand, showed a more linear relationship with crater volume, and the ratio of impulse over crater volume (I/V) remained constant for the entire range of drop sizes, impact velocities, and surface conditions used in this study. Surface shear strength, represented by the penetration depth of fall-cone penetrometer, appeared to be a key factor involved in this process. An equation was developed which related crater volume to cone penetration depth and impact impulse. Crater volume, which appeared to be a better indicator of the total amount of material dislodged by a raindrop than splash amount, can thus be predicted using this equation.

KEY WORDS: raindrop impact; rain erosion; impact erosion; cratering; impact cratering; cavity formation; splash erosion

INTRODUCTION

Single drop impact and photographic studies of the 1970s and 1980s revealed that rain erosion can be divided into three inter-related processes of impact, splash and cratering (Ghadiri and Payne, 1977, 1981). The impact and splash processes have since been studied by many researchers and are well understood (Ghadiri and Payne, 1986, 1988; Al-Durrah and Bradford, 1981, 1982; Nearing *et al.*, 1986, 1987; Nearing and Bradford, 1985, 1987; Sharma and Gupta, 1989). Cratering, or the process of cavity formation by a falling raindrop digging into the soil or other target materials, on the other hand, has not received much attention in soil erosion research. Its mechanism is not known, nor is its role and significance in the processes which lead to the removal and transport of soil material. Even in the field of alloys and metals, erosion under very high (supersonic) impact velocities of raindrops or water sprays where crater formation or target penetration is the main concern, the process is not fully understood (Adler, 1999). A few empirical equations have been developed for the supersonic impact of water drops onto a liquid surface (Engel, 1961, 1962, 1966), water drops onto a solid surface (Pitek & Hammitt, 1966; Rinehart, 1950; Van Valkenburg *et al.*, 1956; Adler, 1991), and solid spheres onto a solid surface (McKenzie *et al.*, 1959; Mihara, 1952; Summer and Charters, 1960), where crater volume has been equated with the energy or some other factors of the impacting drop or projectile. However, the applicability of such equations to cratering in low strength granulated material such as soil by the low velocity impact of free-falling raindrops has not been tested.

Most of the empirical equations developed for supersonic collision of liquid drops with solids relate crater depth, diameter or volume to an exponent of impact velocity. None of these equations contributed significantly to a fundamental understanding of the flow of material under impact which leads to crater formation (Cook, 1959; Engel, 1961; Pitek and Hammitt, 1966). Target strength, as a parameter in these empirical equations, appears to play a secondary role to sound velocity, which is a function of elastic properties of targets. It is not clear why elastic properties affect a process which is dominated by plastic flow.

* Correspondence to: H. Ghadiri, Faculty of Environmental Sciences, Griffith University, Nathan, Queensland 4111, Australia.
E-mail: H. Ghadiri@mailbox.gu.edu.au

The only study of crater formation by the impact of free-falling water drops at near-terminal velocities was carried out some 40 years ago by Engel (1961). This study resulted in the development of the following empirical equation:

$$D = KR(\rho V^{\cdot})^{\frac{1}{3}}$$

in which D is the maximum cavity depth, K is a constant, and V, R and ρ are the velocity, radius and density of the falling drop respectively.

The only study in which crater formation in granulated material by free-falling water drops has been briefly mentioned is the one carried out by Mihara (1952). He found a linear relationship between crater volume and impact velocities higher than 1 m s^{-1}.

This paper reports on a comprehensive investigation into crater formation in soil, sand, pastes of various simple chemicals and water targets by free-falling water drops of different sizes, heights of fall and fall velocities. This study offers a new approach to rain erosion research in which the behaviour of the raindrop and soil surface as the two colliding bodies is considered.

METHODS

Photography

Crater and splash corona formation by the impact of water drops on water targets of various depths, and their eventual collapse was photographed using a high-speed cine photographic technique. The camera used was a Hitachi High Speed Motion Analysis Camera (HIMAC) which is a rotating prism type, having speeds of up to 10 000 pictures per second. The actual speed of the frames on which impact was caught was measured from the timing marks made on the film by a timing device. Filming was carried out through the transparent walls of the container of target water with the camera lens parallel to the water surface. A light-sensitive diode was used as an automatic triggering device, which was coupled with an event synchronizer to delay the actual shooting of the event at a predetermined elapse time following the release of the water drops from the top of a 9 m tall tower. Back-lighting with a 600 watt bulb focused onto the camera lens was used for target illumination.

The films were projected onto large graph papers, stopped on each frame, and the outlines of crater and corona were drawn on the paper. The elapsed time since impact was also determined and recorded on the drawing of each still frame (Figure 1). These drawings were then used to determine the depth and diameter of the crater at various time intervals after impact. The formation, growth and eventual collapse of the splash corona on the rims of the crater were also recorded and measured on these drawings or directly from the projected still frames. The sequences showing the entire processes of crater and corona formation and collapse were prepared by printing one in every 10 to 50 frames after impact and arranging them as shown in Figure 2.

Water drop formation

A full range of glass droppers was made, which were capable of producing drops of 14 to 158 mg (equivalent spherical diameter of 3 to 6·7 mm). The relationship between the diameter of glass jets and that of the drop they form (Laws, 1941) was used for making the droppers capable of producing drops of the required diameters. The drops were released from different heights, ranging from 1 m to 8 m height of fall, at 1 m increments. Drop weight was determined by collecting and weighing 100 drops in a pre-weighed beaker.

Target preparation

Duplicate samples of soil, sand and chemical paste were prepared with a wide range of water contents and used simultaneously, one as a target for water-drop impact and the other for fall-cone penetration. Non-liquid targets were prepared in Petri dishes of known weight and following the landing of a single water drop on the targets splash loss was determined by reweighing the sample. The depth and diameter of the crater formed by water-drop impact were measured immediately following the impacts as discussed below.

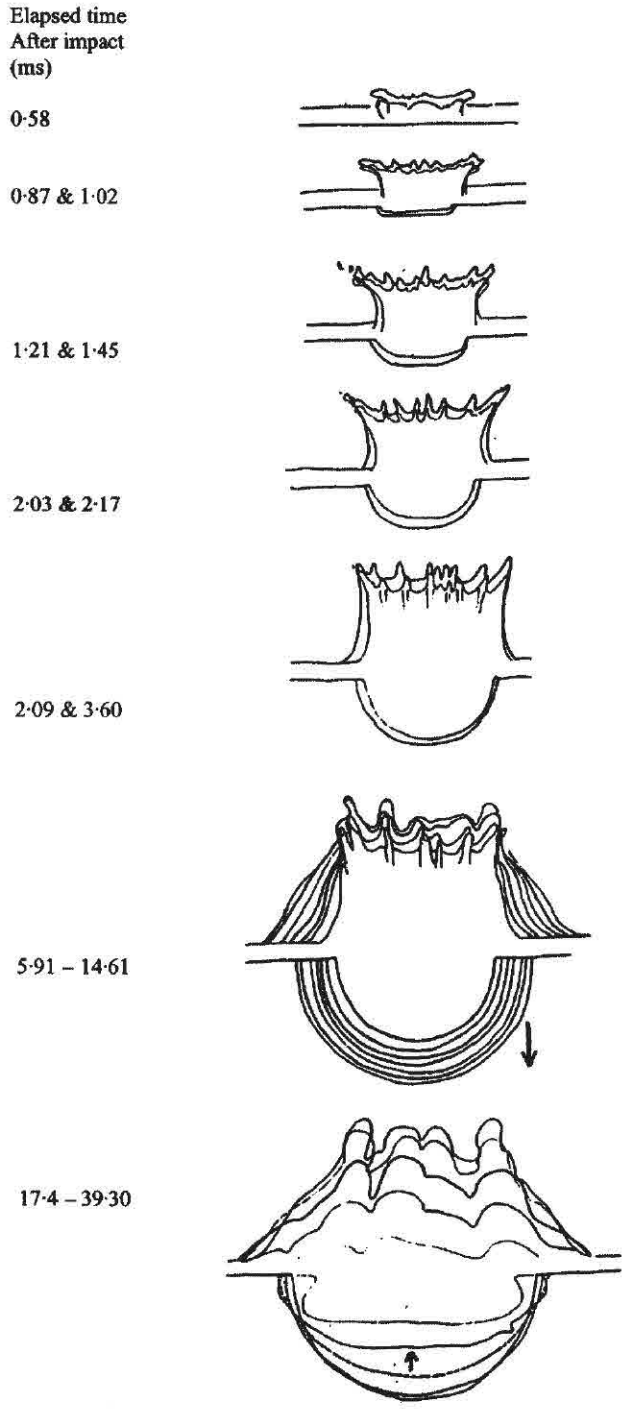

Figure 1. Tracing and measurement of the growth and collapse of craters formed by water drop impacts on water targets

Crater cast penetration

A collection of crater casts was prepared by impacting water drops of various sizes and velocities on different targets and then filling them with a slurry of plaster of Paris. The casts were removed after setting, and were washed, dried and dipped into resin, then their dimensions measured. They were pushed onto the targets on a

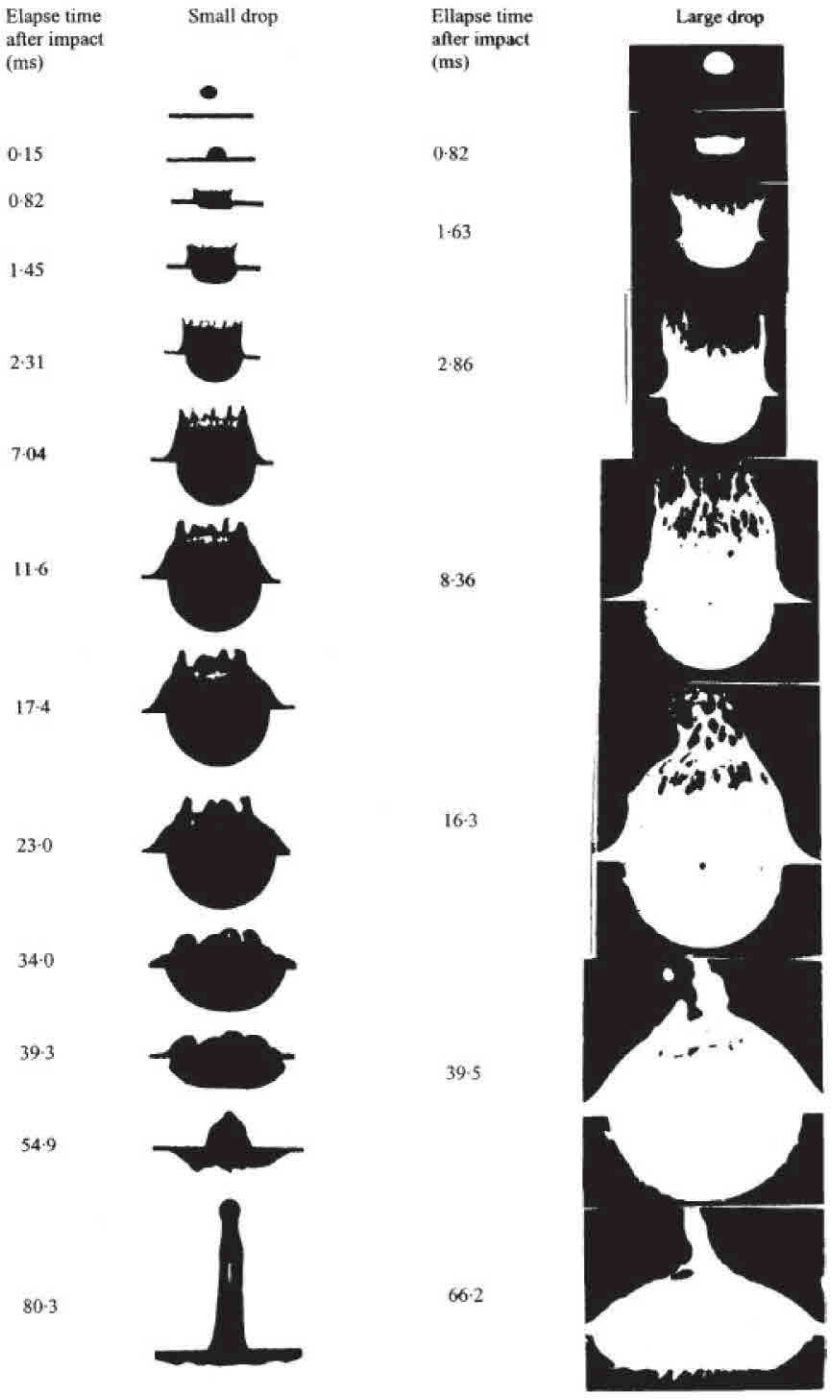

Figure 2. Photographic sequences of crater and corona formation, growth and collapse following the impact of a small drop (left) and a large drop (right) on water targets

top pan balance and maximum load was noted. This load was then converted to force, and then to force per unit area of crater, which was assumed to be equal to target flow stress or static yield strength (Cook, 1959).

Fall-cone penetrometer

A fall-cone penetrometer (Hansbo, 1957) with an automatic release and lock-up system to apply stress for a predetermined duration was used. A range of cones with different weights (24, 80, 130, 180 and 230 g) and angles (30° and 60°) were prepared and used on different targets. Depth of cone penetration was read on the instrument's dial gauge and converted to surface shear strength using equations given in the literature (Hansbo, 1957; Towner, 1973).

Determination of crater area and volume

The depth and diameter of the craters formed on soil, sand and paste target material were measured using a surface profiler, immediately after impact and prior to any drying of the target material and possible shrinkage (Figure 3). Direct measurement of crater dimensions was also carried out for large craters using a micrometer or a ruler. Crater volume (V) and area (S) were calculated using the following equations:

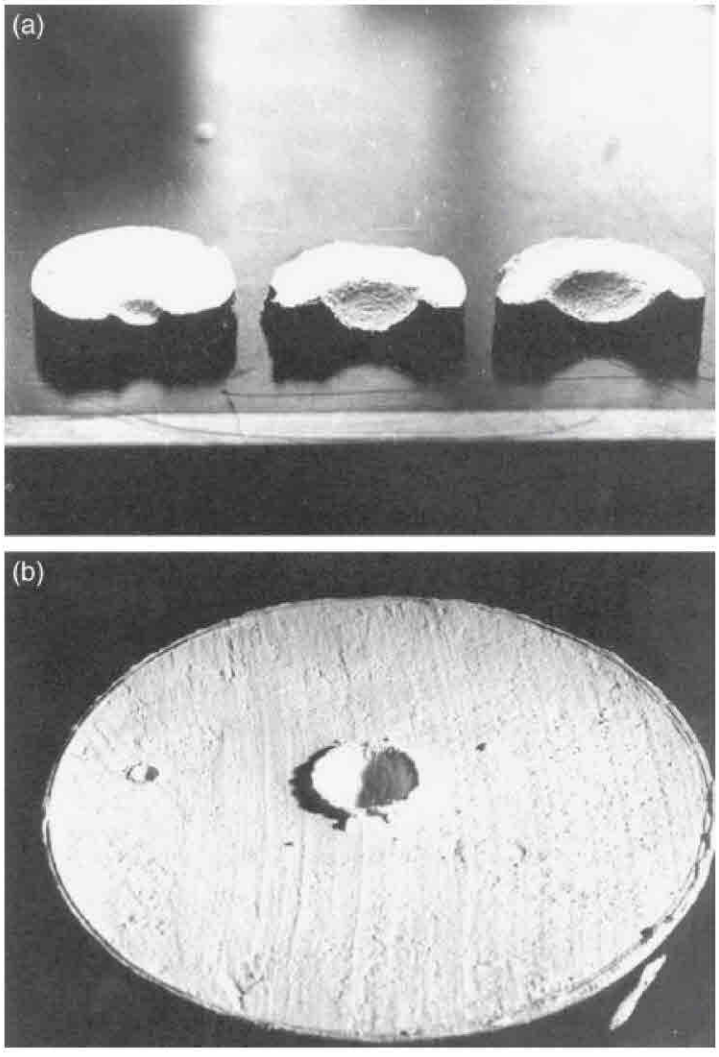

Figure 3. Craters formed in barium sulphate paste by impacting water drops of various sizes and impact velocities

$$V = \frac{1}{3}\pi h^{2}\left(\frac{3d^{2} + 12h^{2}}{8h} - h\right)$$

$$S = \pi\left(\frac{d^{2}}{4} + h^{2}\right)$$

where d and h were crater diameter and depth respectively.

Determination of impact parameters

Drop diameter and its fall velocity were measured photographically. The sections of the films on which the final few milliseconds of falling water drops were captured before hitting the target were projected on large sheets of squared paper and their outlines over a specific number of frames were drawn. The exact diameters of the falling drops were measured from these drawings and their fall velocities were calculated using their displacement with time. Drop mass was determined gravimetrically by collecting and weighing 100 drops in a beaker and determining the weight of one drop. With these three drop parameters known, the values for impact energy ($1/2\, mv^{2}$), momentum (mv), impulse (force $\times$ duration) and stress (ρv^{2}) were calculated.

RESULTS AND DISCUSSION

Crater formation in non-liquid targets

Craters of various shapes and sizes were observed on different solid targets, ranging from circular depressions on unsaturated, compacted soil and sand to almost completely hemispherical shapes on low strength targets. Crater shape depends mainly on the properties of target material, but it is also affected by impact velocity. For the range of non-liquid targets and impact velocities used in the study, craters were mostly in the shape of segments of a sphere (Figures 3 and 4). A completely hemispherical crater was formed on targets of low shear strength such as water (Figure 2).

One of the features of the craters formed in most of the soil and sand targets was the formation of a relatively large rim around them by the deposition of slow-moving target material set in motion towards the end of the splash process (Figures 3–5). This rim makes up the bulk of the rather large difference between crater volume and the volume of splash material and could constitute a large percentage of displaced material. Rim material can take part in the water erosion process and turn into erosion loss if impact is followed by runoff or if the target is on a steep slope. Crater volume, therefore, may be a better indication of soil erodibility and material-displacing capacity of a raindrop, or rain erosivity, than the currently used splash amount.

Cook (1959) found a linear and direct relationship between crater volume and the kinetic energy of an impacting drop at supersonic velocities, and proposed the following semi-empirical equation:

$$V = \frac{\rho_{s}^{1/2}\rho_{d}^{1/2}}{\rho_{s} + \rho_{d}} \times \frac{E_{k}}{2\phi}$$

in which V is crater volume, ρ_{s} and ρ_{d} are target and drop densities, E_{k} is the kinetic energy of the impacting drop, and ϕ is target flow stress. As shown in Figure 6, for most of the targets used in this study, including soils and sands, the relationship between E_{k}/V and impact velocity was non-linear. This relationship appeared to indicate a decrease in the efficiency of impact energy in moving target material at higher velocities. It can therefore be deducted that, as has been the case with the other two impact processes of splash and soil aggregate breakdown (Ghadiri and Payne, 1977, 1979, 1980, 1981), impact energy may not be an important factor in the cratering process. Energy-based equations given by Cook (1959), Engel (1966) and others are therefore not applicable to low velocity impact on low strength solids, but the basic theoretical assumptions upon which they have been developed seem relevant to the present study.

In order to determine the fraction of impact energy which is directly involved in crater formation, a series of cratering experiments was carried out, followed by the static loading of the same targets with a crater cast.

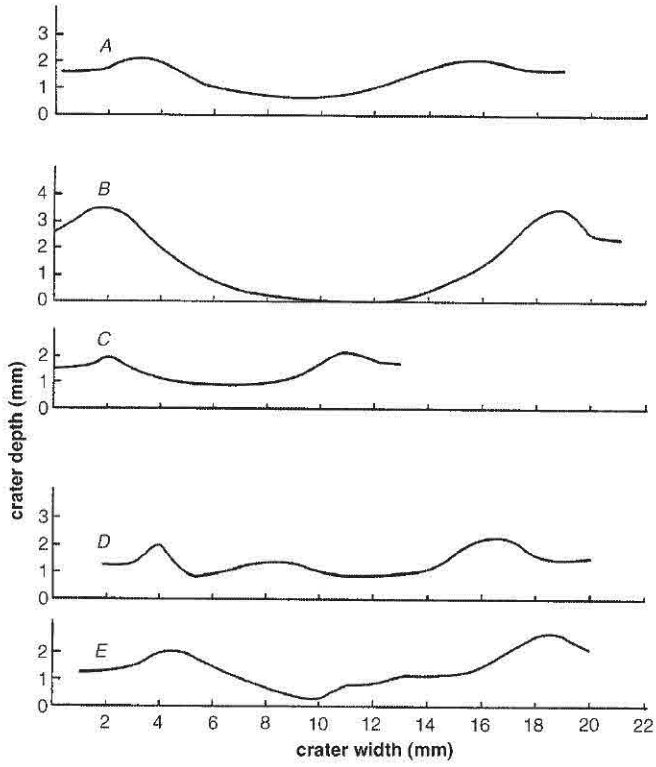

Figure 4. Outlines of the craters formed on some of the target materials used in this study: (A) large drop on saturated fine sand; (B) large drop on soil paste; (C) small drop on soil paste; (D) large drop on dry soil; (E) large drop on wet soil

Table I. Determination of cratering energy by static loading of two barium sulphate pastes (rim included)

Bulk density = 2·07 g cm^{-3}, σ = 0·15 N cm^{-3}, 126 mg drop – different heights of fall					Bulk density = 1·97 g cm^{-3}, σ = 0·086 N cm^{-3}, 4 m height of fall – different drops					
Impact velocity (m s^{-1})	KE (mJ)	Static load (g)	Cratering energy		Drop mass (mg)	Impact velocity (m s^{-1})	KE (mJ)	Static load (g)	Cratering energy	
			Amount (mJ)	% of total					Amount (mJ)	% of total
430	1·21	38	0·25	21	21·7	6·90	0·51	10·1	0·11	22
592	2·30	48	0·53	23	38·8	7·25	1·03	13·2	0·15	14
697	3·18	60	0·65	20	46·5	7·35	1·25	20·0	0·22	18
820	4·40	62	0·76	17	88·1	7·60	2·54	34·2	0·35	14
860	4·84	68	0·90	19	96·0	7·65	2·81	37·0	0·42	15
					112·5	7·70	3·34	39·0	0·45	13
					130·3	7·75	3·92	43·0	0·56	14
					136·0	7·78	4·11	47·0	0·65	16
					156·0	7·80	4·62	56·0	0·79	17

Penetration weight was converted to cratering energy by assuming force per unit area of crater to be equal to the product of target density and square of impact velocity (ρV^2). Results given in Table I show that, depending on target material, between 13 and 23 per cent of impact energy is directly involved in the cratering process. With up to 23 per cent of impact energy involved in cratering, this process appears to be a major user of impact energy. This may explain why so many researchers have found a direct relationship between impact energy

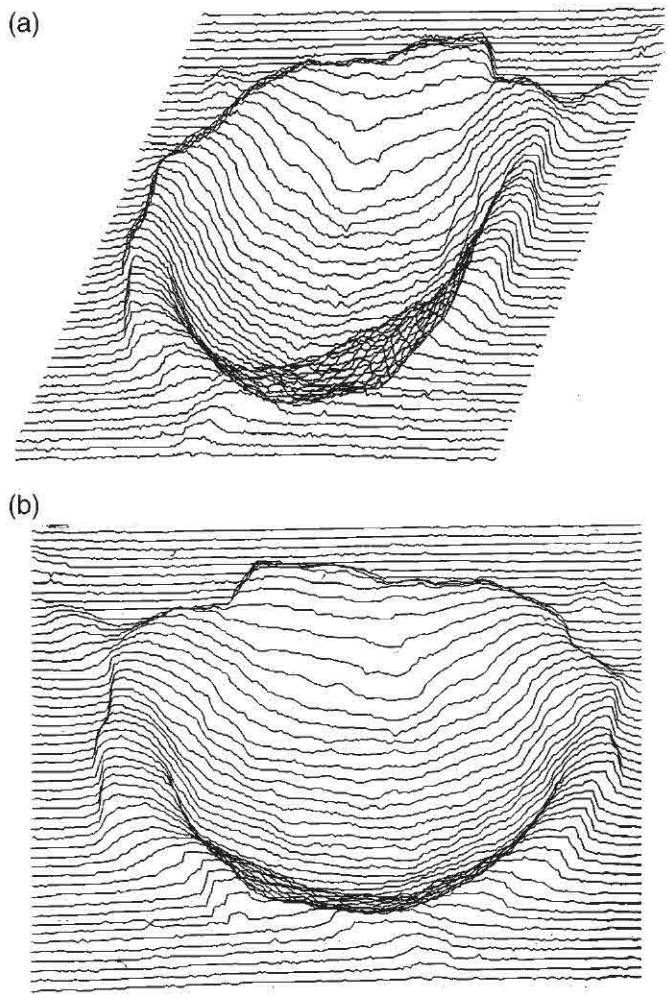

Figure 5. Measurement of crater dimensions using a surface profiler

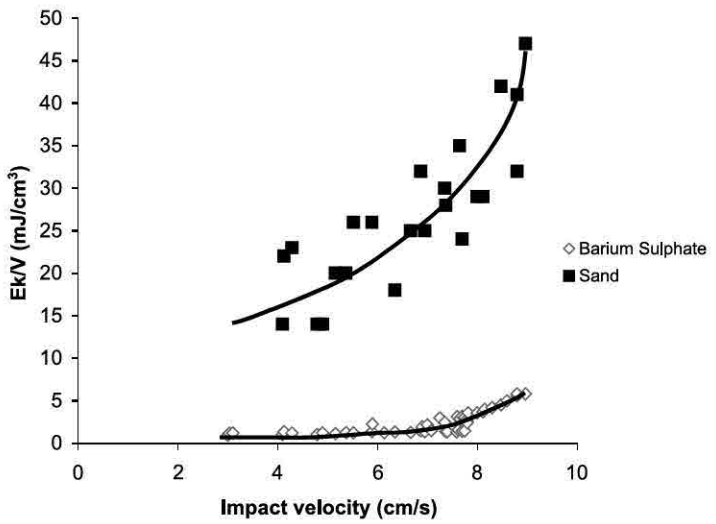

Figure 6. Variations in energy per unit crater volume with impact velocity

Table II. The relationship between crater volume and impact energy, force and impulse on two barium sulphate pastes (drop mass = 126 mg, height of fall = 1–6 m)

Impact velocity ($m\ s^{-1}$)	$BaSO_4$ 33% water $d = 2{\cdot}33\ g\ cm^{-3}$, $P = 14{\cdot}0$ mm			$BaSO_4$ 40% water $d = 2{\cdot}19\ g\ cm^{-3}$, $P = 27{\cdot}9$ mm		
	Crater volume (cm^3)	$\frac{KE}{Vo}$ ($mJ\ cm^{-3}$)	$\frac{I}{Vo}$ ($N\ m^{-3}\ s^{+1}$)	Crater volume (cm^3)	$\frac{KE}{Vo}$ ($mJ\ cm^{-3}$)	$\frac{I}{Vo}$ ($N\ m^{-3}\ s^{+1}$)
4·30	0·058	19·1	173·3	0·184	6·0	63·7
5·90	0·108	19·3	146·0	0·369	5·7	51·3
6·90	0·105	27·0	164·3	0·398	7·2	54·2
7·70	0·097	36·7	193·8	0·513	6·9	50·6
8·25	0·122	33·4	171·9	0·481	5·5	56·4
8·60	0·136	32·7	162·6	0·496	8·9	57·0
8·80	0·122	38·1	184·0	0·576	8·1	52·0
9·00	0·147	35·0	159·8	0·655	7·4	49·0

d, target density; P, depth of cone penetration.

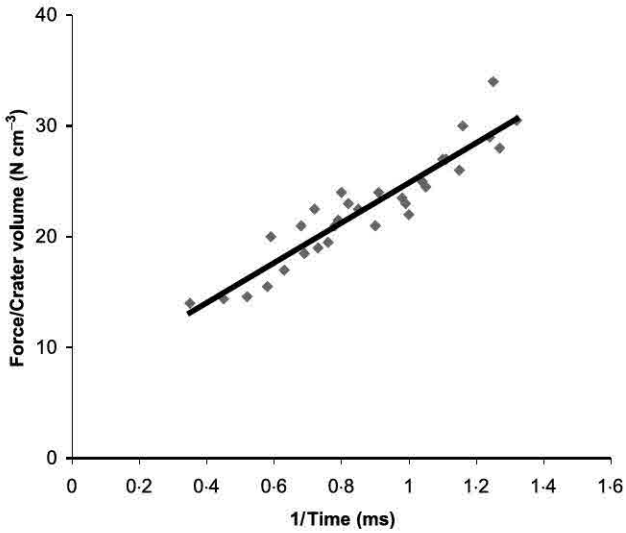

Figure 7. Effect of impact duration on force per unit volume of crater

and crater volume (Cook, 1959; Engel, 1962; Rinehart, 1950; Van Valkenburg *et al.*, 1956). However, the non-linearity of such a relationship, shown in Figure 6, indicates that impact energy may not be the most important single impact factor in cratering and indeed in the entire rain erosion process. It has been shown that the splashing of water droplets and target material uses less than 5 per cent of the impact energy (Ghadiri and Payne, 1979).

Other impact factors whose roles in crater formation were investigated are impact stress, force and impulse (Table II). The results show that stress force and energy per unit volume of crater show more or less the same variation with the impact velocity, but when the effect of time (i.e. impact duration) is taken into account, which converts force to impulse, the results, (I/V), are much more independent of drop size and impact velocity (Table II). Two factors shown by Ghadiri and Payne (1979) to be closely related to splash amount, i.e. force and time, also show a closer relationship with crater volume than any other single or combined impact factors. There is a linear relationship between force per unit crater volume (F/V) and the reciprocal of time during which force is acting on the surface (Figure 7).

Stress concentration around the periphery of an impacting drop, as reported by Ghadiri and Payne (1981), did not seem to have any bearing on the cratering process, possibly because the crater was largely formed under the prolonged lateral target stress, which followed the initial short-lived compressive or circumferential high pressure and remained effective throughout the cratering process. Circumferential high pressure could well have left some marks on the target, but all such marks were removed later during target flow and the crater formation process which followed.

In order to investigate the effect of the target factor involved in cratering, static loading of targets by crater casts was carried out for a number of targets. The following empirical model best fitted the experimental results:

$$V = \frac{\rho_{\cdot}\rho_{\cdot}}{\rho_{\cdot} + \rho_{\cdot}} \times \frac{E_{\cdot}}{2\phi} \tag{1}$$

Mean force per unit area of crater, together with crater volume and target density, were put into this equation and the energy applied by the crater cast calculated. Results showed a good agreement between the energies worked out in this way and those calculated through mass and velocity of impacting drops. The only significant point which this agreement suggests is that it is possible to estimate a dynamic property of target material, i.e. flow stress, by a simple method of static loading which measures static yield strength. Results also suggest that target density was not an important factor in cratering, and flow stress might in fact be the only target factor involved in this process.

Fall-cone penetration – crater volume relationship

Following the measurement of flow stress by static loading, it was decided to examine the use of a fall-cone penetrometer instead of crater cast, since it has many advantages over the cast method, including constant and repeatable loading, adjustable cone weight, and exact duration of loading.

Cone penetration experiments were carried out on various targets of different densities and flow stresses. Duplicates of the same targets were exposed to falling water drops of different sizes and fall velocities simultaneously. These experiments also showed that the ratio of impact energy over crater $E_{\cdot}/V$ increased with impact velocity, but impulse per unit crater volume (I/V) was constant for each target in almost all the cases studied, supporting the results obtained by crater cast method. Mean I/V and cone penetration depth for different targets are given in Table III. These results show an inverse relationship between I/V and the square of cone penetration depth ($P^{\cdot}$). The products of I/V and $P^{\cdot}$ show only random variation throughout the range of targets used. Target density had no effect on this relationship. The relationship was as follows:

Table III. Relationship between crater volume and depth of cone penetration

Target material	Water content (%)	Bulk density (kg m$^{-\cdot}$)	Material density (kg m$^{-\cdot}$)	Mean cone penetration (P) (mm)	Mean impulse / Vo (N m$^{-\cdot}$ s)	$\frac{I}{Vo} \times P^{\cdot}$ ((N m$^{-\cdot}$ s) $\times 10^{\cdot}$)
Soil paste, Class 5	55	1640	2600	28·3	83·4	667·9
Barium sulphate	40	2190	4500	27·8	55·6	429·7
Soil paste, Class 8	75	1540	2600	23·1	113·0	613·7
Fine sand	29	1800	2600	23·0	125·0	661·3
Barium sulphate	36	2230	4500	18·5	104·5	357·7
Soil paste, Class 1	65	1600	2700	18·0	184·2	596·8
Soil paste, Class 8	70	1570	2600	17·3	276·4	827·2
Red lead oxide	20	3840	9100	15·4	137·8	326·7
Soil paste, Class 8	66	1600	2600	15·2	316·3	730·8
Barium sulphate	33	2400	4500	14·1	169·5	337·0
Soil agg., Class 5	Sat.	1440	2600	13·7	196·7	369·2
Medium sand	25	1890	2600	13·3	218·6	386·7
Soil paste, Class 1	58	1640	2700	11·6	454·1	611·0
Soil paste, Class 1	55	1660	2700	9·5	733·6	662·1

$$\frac{I}{V} = K\frac{1}{p^{\wedge}} \tag{2}$$

where K is a proportionality factor whose value depends on the cone weight and the duration of cone penetration. By separating these two factors and individually representing them, the equation becomes:

$$\frac{I}{V} = k\frac{M}{t} \times \frac{I}{p^{\wedge}} \tag{3}$$

where M is cone mass (in grams), t is the duration of cone penetration (in seconds) and k is a non-dimensional constant. This is an empirical equation, but it is dimensionally balanced and it has some theoretical plausibility. The right-hand side of Equation 3 is similar to what Hansbo (1957) considers to be equal to target shear strength. Thus:

$$\frac{I}{V} = \tau \quad \text{or} \quad \frac{I}{\tau} = V \tag{4}$$

which means that cratering is a function of drop impulse and target shear strength with no involvement of other target or drop factors. This is compatible with cratering being mainly a shear flow process with little or no compaction or other forms of deformation processes involved.

By inserting values for M, t and $(I/V) \times P^{\wedge}$ in Equation 3 for this particular set of experiments, $k = 1052$ and Equation 3 becomes:

$$V = 1{\cdot}95 \times 10^{-3} IP^{\wedge} \tag{5}$$

Plotting logarithm of I/V against logarithm of $P^{\wedge}$ for the data given in Table III resulted in a linear relationship with the following regression equation (Figure 8):

$$\mathrm{Log}\left(\frac{I}{V}\right) = 3{\cdot}72 - 1{\cdot}0648 \log P^{\wedge} \tag{6}$$

It can also be expressed as:

$$V = 1{\cdot}91 \times 10^{-3} IP^{\wedge -1{\cdot}1} \tag{7}$$

which is very similar to Equation 5. The slight difference between Equations 5 and 7 is probably due to insufficient data from which the regression equation was derived.

Equation 5 and its more specific form, Equation 7, apply reasonably well for the range of targets and impact velocities used in this study and may also apply to other conditions. Equation 3 offers a new and simple means

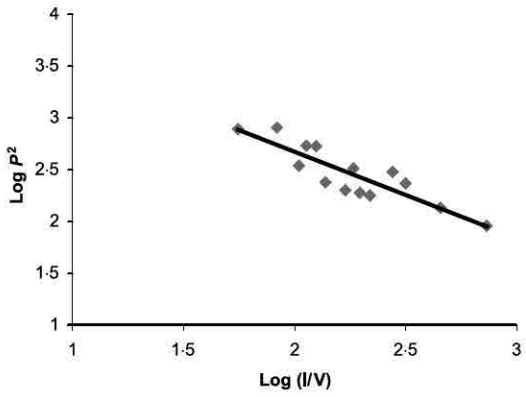

Figure 8. Relationship between depth of cone penetration and the ratio of I/V

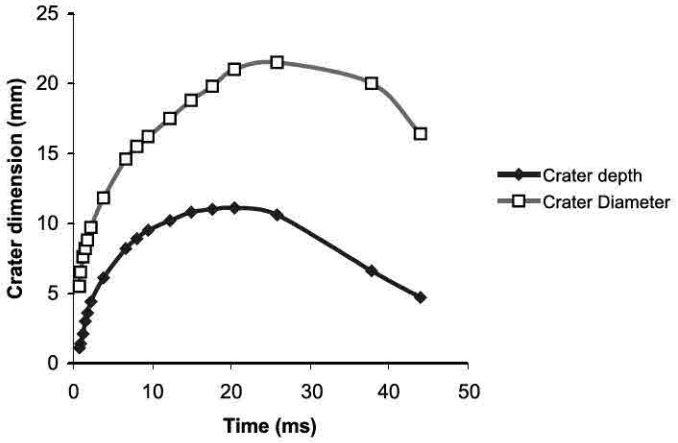

Figure 9. Changes in crater depth and diameter with time in water target (drop diameter = 3·5 mm, impact velocity = 5·7 m s^{-1})

for soil characterization and the prediction of soil erodibility, but more work is required to evaluate the findings under multiple-drop impact of natural or simulated rain and to make use of the proposed methods and equations in the field.

Crater formation in liquid targets

Crater formation in liquid targets was studied photographically on targets of water and of dense solutions. Figure 2 shows two of the sequences prepared from the films taken from the impact of large and small drops on water. Craters at their maximum depth were all hemispherical in shape, and depth never exceeded one-half of the diameter. Plots of crater depth and diameter versus time shown in Figure 9 appear to be parts of a family of ellipses tangential to the crater dimension axis at the origin and fit the general equation for a family of ellipses. The change in crater diameter with time showed marked differences with large and small drops. The diameter of the crater formed by large drops increased indefinitely with time (eventually turning into ripples). Those formed by small drops reached a maximum at about the same time as the maximum time was reached and then began decreasing to form a tall Raleigh jet (Figure 2).

Figures for maximum crater depth and its corresponding diameter were used for the calculation of crater volume. Cratering duration, and I/V were calculated in the same way as for non-liquid targets. Results agreed with the conclusions reached for cratering on non-liquid targets. Variations among I/V values were random and negligible, while E_i/V increased with impact velocity. Target density had no effect on I/V as with non-liquid targets.

CONCLUSION

Craters formed by raindrop impacts on different soils or other low strength materials differ significantly in depth, diameter and shape but crater volume remains reasonably constant. Impact cratering appears to be a function of impact impulse and target shear strength with little involvement of other target or drop factors. The penetration depth of Hansbo's fall-cone penetrometer was successfully used to represent target shear strength in an equation developed to predict crater volume, or total material displacement, by single drop impact. In this equation rain erosivity is represented by impact impulse. The equation appears to apply to water targets as well as solid materials. Crater volume may be a better indicator of impact erosion than the commonly measured splash amount.

REFERENCES

Adler WF. 1991. Supersonic waterdrop impacts on materials. *Proceedings of the 6th European Electromagnetic Structure Conference*. Friegrichshafen: 237–245.

Adler WF. 1999. Rain impact retrospective and vision for the future. *Wear* **233–235**: 25–38.

Al-Durrah MM, Bradford JM. 1981. New method of studying soil detachment due to waterdrop impact. *Soil Science Society of America Journal* **45**: 949–953.

Al-Durrah MM, Bradford JM. 1982. Parameters for describing detachment due to single waterdrop impact. *Soil Science Society of America Journal* **46**: 836–840.

Cook MA. 1959. Mechanism of cratering in ultra-high velocity impact. *Journal of Applied Physics* **30**: 725–735.

Engel OG. 1961. *Collision of liquid drop with liquids*. Technical Note 89. National Bureau of Standards.

Engel OG. 1962. *Crater depth in fluid impacts*. WADD-TR-60-475 part 2. Aeronautical Systems Division of National Bureau of Standards, UK.

Engel OG. 1966. Crater depth in fluid impacts. *Journal of Applied Physics* **37**: 1798–1808.

Ghadiri H. 1988. The formation and characteristics of splash following raindrop impact on soil. *Journal of Soil Science* **39**: 563–575.

Ghadiri H, Payne D. 1977. Raindrop impact stress and the breakdown of soil crumbs. *Journal of Soil Science* **28**: 247–258.

Ghadiri H, Payne D. 1979. Raindrop impact and soil splash. In *Soil Physical Properties and Crop Production in the Tropics*, Greenland DG, Lal R (eds). John Wiley and Sons: London; 95–105.

Ghadiri H, Payne D. 1980. A study of soil splash using cine-photography. In *Assessment of Erosion*, DeBoodt MF, Gabriels MD (eds). John Wiley and Sons: London; 185–192.

Ghadiri H, Payne D. 1981. Raindrop impact stress. *Journal of Soil Science* **32**: 41–49.

Ghadiri H, Payne D. 1986. The risk of leaving soil surface unprotected against falling rain. *Journal of Soil and Tillage Research* **8**: 119–130.

Hansbo S. 1957. *A new approach to the determination of the shear strength of clay by fall-cone test*. Royal Swedish Geotechnical Institute, Proc. No. 14.

Laws JO. 1941. Measurement of the fall velocity of water drops. *Transactions of the American Geophysical Union* **22**: 709–721.

McKenzie RJ, Martin FF, Kenworth HM. 1959. High velocity impact of small metal spheres upon flat targets. *Proceedings of 3rd Hypersonic Impact Symposium* **1**: 249–255.

Mihara Y. 1952. *Raindrop and soil erosion*. Bulletin of the National Institute of Agricultural Science Japan, Series A, No. 1.

Nearing MA, Bradford JM. 1985. Single waterdrop detachment and mechanical properties of soils. *Soil Science Society of America Journal* **49**: 547–552.

Nearing MA, Bradford JM. 1987. Relationship between waterdrop properties and forces of impact. *Soil Science Society of America Journal* **51**: 425–430.

Nearing MA, Bradford JM, Holtz RD. 1986. Measurement of force vs. time relations for waterdrop impact. *Soil Science Society of America Journal* **50**: 1532–1536.

Nearing MA, Bradford JM, Holtz RD. 1987. Measurement of waterdrop impact pressures on soil surfaces. *Soil Science Society of America Journal* **51**: 1302–1306.

Pitek MJ, Hammitt FG. 1966. *Hyper-velocity and fluid impact studied; A literature review*. Technical Report No. 1, College of Engineering, University of Michigan.

Rinehart JS. 1950. Some observations on high-speed impact. *Popular Astronomy* **58**: 458–464.

Sharma PP, Gupta SC. 1989. Sand detachment by single raindrops of varying kinetic energy and momentum. *Soil Science Society of America Journal* **53**: 1005–1010.

Summers JL, Charters AC. 1969. High-speed impact of metal projectile in targets of various material. *Proceedings of 3rd Hypersonic Impact Symposium* **1**: 101–113.

Towner GD. 1973. An examination of the fall-cone method for the determination of some strength of remoulded agricultural soils. *Journal of Soil Science* **24**: 470–479.

Van Valkenburg ME *et al*. 1956. Impact phenomena at high speed. *Journal of Applied Physics* **27**: 1023–1028.